

**Motion correction of Single Voxel Spectroscopy by Independent Component Analysis  
applied to spectra from non-anesthetized pediatric subjects**

Robin de Nijs<sup>1,2</sup>, MSc PDEng, Maria J. Miranda<sup>1,3</sup>, MD PhD

Lars Kai Hansen<sup>4</sup>, MSc PhD, Lars G. Hanson<sup>1</sup>, MSc PhD,

1. Danish Research Centre for Magnetic Resonance, Hvidovre, Denmark
2. Neurobiology Research Unit, Copenhagen, Denmark
3. Department of Pediatrics, Copenhagen University Hospital Hvidovre, Denmark
4. Technical University of Denmark, Department of Informatics and Mathematical modeling, Lyngby, Denmark

Full paper

Word count of manuscript body: 4623

Running title: *Motion correction of SVS from pediatric subjects by ICA*

Correspondence:

Robin de Nijs

Danish Research Centre for Magnetic Resonance

Department of MR, Section 340

Copenhagen University Hospital Hvidovre

Kettegaard Allé 30

DK-2650 Hvidovre

Denmark

Tel: +45 3632 2885

Fax: +45 3647 0302

E-mail: [rdenijs@drcmr.dk](mailto:rdenijs@drcmr.dk)

## **Abstract**

For Single Voxel Spectroscopy (SVS), the acquisition of the spectrum is typically repeated  $n$  times and then combined with a factor  $\sqrt{n}$  in order to improve the Signal-to-Noise Ratio (SNR). In practice the acquisitions are not only affected by random noise, but also by physiological motion and subject movements. Since the influence of physiological motion such as cardiac and respiratory motion on the data is limited, it can be compensated for without data-loss. Individual acquisitions hampered by subject movements on the other hand need to be rejected, if no correction or compensation is possible. If the individual acquisitions are stored, it is possible to identify and reject the motion-disturbed acquisitions before averaging.

Several automatic algorithms were investigated using a dataset of spectra from non-anesthetized infants with a gestational age of 40 weeks. Median filtering removed most subject movement artifacts, but at the cost of increased sensitivity to random noise. Neither Independent Component Analysis (ICA) nor outlier identification with multiple comparisons has this problem. These two algorithms are novel in this context. The peak height values of the metabolites were increased compared to the mean of all acquisitions for both methods, although primarily for the ICA method.

Keywords: *single voxel spectroscopy, motion correction, ICA, proton spectroscopy*

## **Introduction**

Subject movement during consecutive Single Voxel Spectroscopy (SVS) acquisitions is often not detected and the resulting distorted data affects the outcome measures. Since severe patient movements, as present for instance in SVS of non-anesthetized pediatric patients, psychiatric and demented patients, cause significant deterioration in spectra, they should not be ignored. For example, movements may introduce a bias in a comparative study between patients and healthy controls. Despite its significance, the issue of identifying motion-distorted spectra, in contrast to motion correction and compensation, is quite unexplored and often not mentioned (1, 2).

Compensation for spectra that are potentially affected by physiological motion can be performed by cardiac and respiratory gating (3) and/or breath holding techniques (4). Since disturbances in phase and frequency by physiological motion are limited (5), they can be compensated for by phase correcting the individual acquisitions before averaging, a process known as phase coherent or constructive averaging (6), followed by frequency shift correction (7, 8). However these techniques can potentially introduce a bias caused by differences in noise between subjects. A bias towards increased phase reference signals may also result.

Severe patient movement cannot be compensated for and the acquisitions distorted by patient motion need to be identified and rejected. Motion can be tracked by a water-signal-based navigator (9), or an interleaved navigator scan (10). Especially J-difference editing is sensitive to motion artifacts and it was shown that the interleaved navigator scan is sufficient (11).

However, a navigator scan is not necessarily needed since the single voxel spectra of the consecutive acquisitions reveal information of the subject's movement. The motion-distorted acquisitions seem easy to identify visually, but commonly used “objective” rejection criteria are typically based on the position, amplitude and width of the suppressed water peak and an arbitrary threshold (12). Alternatively a cluster analysis of the lipid signals can be used to correct for subject motion (13), but a lipid signal might not always be present.

In practice, motion correction consists of two steps. First the acquisitions severely deteriorated by subject movements need to be identified and excluded. Second the remaining acquisitions need to be frequency-shifted and phase-corrected individually (13).

Movements during an individual acquisition, and severe movements between acquisitions, may corrupt the entire spectrum of the acquisition irreversibly. Limited movement between individual acquisitions will introduce a simultaneous broadening and lowering of the peak in the mean

spectrum but keeping the area under the peak approximately constant. This can affect the output of the fitting procedure, if peak shapes are assumed. Movement can also result in a different location of the measured volume, which additionally can cause an error in metabolite concentrations if these vary with position. There can be a difference between the group of patients and the healthy controls regarding unrecoverable subject movements. The patient data might suffer more from subject movements, and if no movement compensation is performed, this will cause a systematic underestimation of metabolites in this group and thus introduce a bias in the study (7).

Corrections primarily have to ensure robust positioning of the measured volume while keeping the signal free of motion-induced bias, and secondarily keeping the noise low and the Signal-to-Noise Ratio (SNR) as high as possible. SNR is typically increased compared to conventional averaging by phase-coherent averaging (14) and also potentially by outlier rejection techniques due to the unwanted contributions to the motion-distorted signal.

Here, subject movement is demonstrated to be a severe problem for non-anesthetized infants. Several algorithms for identifying and rejecting motion-corrupted spectra were implemented and compared.

## **Materials and methods**

### *Subjects and data acquisition*

Subjects were infants born at the Copenhagen University Hospital, Hvidovre, Denmark, and taking part in a MRI/MRS-preterm infant cohort study. The study includes data from 97 infants; 77 preterm infants (prematurely born between 12 and 6 weeks before term) and 20 controls (born at term). All infants were MR-scanned around term or term-equivalent age, and were not anesthetized before or during scanning. The local ethics committee accepted the study and informed parental consent was obtained in all cases.

MR scanning was performed on a Magnetom Trio 3 tesla scanner (Siemens, Erlangen, Germany) with a quadrature single channel head coil. An 8 mL cubic voxel was placed in the posterior periventricular white matter, by the posterior horn of the lateral ventricles, and a 3.4 mL cubic voxel was placed at the level of the basal ganglia and thalami, both randomly positioned in the right or left hemisphere. For each voxel position 48 Free Induction Decay signals (FIDs) based on two phase-cycled averages, each with 1024 complex points and a readout period of 850 ms,

were acquired with a Point RESsolved Spectroscopy (PRESS) sequence (15) for two echo times (30 and 144 ms) with a repetition time of 2 seconds.

For every subject, four datasets of 48 repetitions each were acquired for the two different voxels and the two echo times. In order to investigate the effect of subject movement under more controlled conditions a healthy volunteer was scanned with the same sequences with 30 ms echo time and same position and size of the 8 mL cubic voxel. The complete measurement of the volunteer with 48 acquisitions was repeated three times. The volunteer was instructed to lie motionless during the acquisition of the first dataset and instructed through the intercom to move his head a few centimeters to the left and right for a few seconds approximately at every 16th acquisition of the last two datasets.

Datasets where all 48 repetitions contained severely corrupted measurements, or where water suppression failed, were excluded from this comparative study after visual inspection of the spectrogram. This resulted in 130 datasets (64 with long echo time) for an 8 mL voxel and 113 datasets (56 with long echo time) for a 3.4 mL voxel. From the 130 datasets with an 8 mL voxel and from the 113 datasets with a 3.4 mL voxelsize, 30 and 26 datasets respectively originated from term infants. The resulting mean or median spectra are zero-order phase-corrected and filtered with a first order Gaussian low pass filter with a full width at half maximum of 1 Hz. Spectra were frequency adjusted based on the position of the N-acetyl aspartate (NAA), creatine (Cr) and choline (Cho) peak, at 2.02 ppm, 3.04 ppm and 3.24 ppm, respectively. Phase-coherent averaging was not applied.

Since the motion-distorted acquisitions are visible as shifts in the frequency domain, it is natural to perform the motion rejection in this domain. It is also possible to carry out the analysis on the Free Induction Decay (FID) signal in the time domain (16), but this has not been done in this study.

The performance of three classes of subject-movement-rejection algorithms was investigated: 1. Simple median filtering, which provides a more robust but more noise sensitive estimate than mean filtering. 2. An outlier identification (OI) algorithm with and without multiple comparisons. 3. Independent Component Analysis (ICA), where the main component represents the spectrum least affected by motion. Corrections as described in the introduction (6, 7, 10, 14) were not performed. Focus was on identification and rejection of the corrupted acquisitions within a dataset.

### *Mean and median filtering*

In the conventional way of data processing, all spectra are averaged permitting motion-distorted acquisitions to degrade the final spectrum. One way of dealing with this problem is to reduce the influence of outliers by median filtering (17, 18). Instead of using the mean as a signal estimator, the median is used and this provides a more robust estimate. The mean minimizes the expectation value of the squared deviation, i.e. the variance, while the median minimizes the expectation value of the absolute deviation. This means that the influence of outliers is reduced. An appealing property of the median is that the shift does not depend on the numerical value of the outlier; only the position of the median in the list of ordered samples is shifted half a position. In the case of an even number of outliers symmetrically spread around the true mean value, the shift is even cancelled.

The noise  $N$  is defined as the standard deviation of the signal estimator. For a dataset  $x_i$  with  $n$  samples, mean  $\bar{x}$ , median  $\tilde{x}$ , standard deviation  $\sigma$  and probability function  $p(x)$  the noise is given by

$$N_{\text{mean}}^2 = \frac{\sigma^2}{n}, \quad N_{\text{median}}^2 \approx \frac{1}{4 \cdot n \cdot p^2(\tilde{x})} = c^2 \cdot N_{\text{mean}}^2, \quad (1)$$

where  $c$  is the efficiency of the mean relative to the median, which is  $\sqrt{\pi/2}$  and  $\sqrt{3}$  for a normal distribution and uniform distribution, respectively. The approximation of the noise for the median holds for large sample sizes with an arbitrary probability function (19, 20). The probability function of the median is normally distributed for any probability function of the samples. Median filtering (together with minimum and maximum filtering) is a well-known type of order-statistics filtering (21).

Since spectra are complex, the average and the median of both the real and imaginary part were calculated separately.

### *Outlier identification*

Outliers can be identified and excluded by an approximation of the standard deviation and a t-test. Performing this outlier identification and rejection for every single frequency (pointwise outlier identification) will reduce the contribution of outliers. In this context a novel alternative is

to reject a whole acquisition, if only one Fourier component is identified as an outlier (outlier identification). It is assumed that the acquisitions without outliers are normally distributed. The significance level  $p$  for the first method was arbitrarily chosen at 5% double sided, i.e.  $z_{\max}=1.96$ , where  $z$  is the  $z$ -score, which is defined by the difference from the mean measured in the number of standard deviations. The significance level for the second method is corrected for multiple comparisons and this was arbitrarily chosen at 10% (double sided) divided by the number of data points (=1024) for one acquisition, i.e.  $z_{\max}=3.9$ . Since the outliers were included in the calculation of the standard deviation, the procedure needs to be repeated in an iterative fashion. The first (crude) estimation of the outlier-free signal is given by the mean and the standard deviation of all samples  $x_i$ . The next estimates, denoted  $x^*$  with iteration number  $j$  are calculated in an iterative fashion (22) with

$$x_{j+1}^* = \bar{x} \text{ and } \sigma_{j+1}^2 = \overline{(x_{j+1}^* - x_i)^2} \text{ for all } x_i \text{ with } |x_i - x_j^*| < z_{\max} \cdot \sigma_j, \quad (2)$$

until convergence is reached. An iterative t-test has never been applied before in this context, but the idea behind the method is similar to the iterative f-test algorithm described by Andersson (23).

### *Independent Component Analysis (ICA)*

Independent Component Analysis (ICA) supplies a mathematical framework for analysis of a group of acquisitions. The method (24) is implemented as a toolbox<sup>1</sup> (25) in Matlab (Mathworks). ICA is a set of methods for blind signal separation, each method sharing the assumption that two arbitrary components are statistically independent (26). Blind signal separation refers to the common situation in signal processing in which we aim to separate unknown source signals from an unknown mixture. Another way of describing or defining ICA is by minimizing the mutual information between the components.

With index  $i$  denoting the acquisition number, and the index  $j$  denoting the component number, the dataset consisting of  $n$  acquisitions  $x_i(t)$  is described by  $M$  components  $s_j(t)$  with coefficients  $a_{ij}$  with

$$x_i(t) = \sum_{j=1}^M a_{ij} \cdot s_j(t) + \text{noise}. \quad (3)$$

Since the ICA algorithm only works for real signals, the complex spectrum is transformed into a real signal by adding the imaginary amplitude spectrum behind the real spectrum. An important complication that often arises in practical applications is that the number of components  $M$  is unknown. Using a Bayesian ICA formulation, this problem can be solved in the limit of many acquisitions (27, 28). The Bayesian Information Criterion (BIC) selects the number of components by estimating the probability of the model containing  $M$  components given the observed data  $p(M)$ , where the number of components is varied in a range from 1 to  $M_{\max}$  (the maximum number of components was set to 12). The signal variance not accounted for by the  $M$  components is assumed to be contributed by an additive normal independent identically distributed white noise signal component (the BIC selection of the number of components is included in the toolbox (25)). Checks are performed to see if the probability for the number of components is less than 50%.

In the case of a dataset without distorted spectra, ICA will find one component representing the underlying spectrum. The difference between the spectra reconstructed with this component and the measured spectra equals the noise as identified by the ICA algorithm.

If the ICA algorithm finds more than one component, the independent component representing the undistorted spectrum needs to be identified, since ICA does not assign a clear meaning to its components. The dominant component of every single acquisition is determined and the acquisitions with the dominant component equal to the most frequent dominant component (the main component) for all acquisitions are considered to be a measurement of the undistorted spectrum. No arbitrary thresholds need to be set. The ICA method produces three spectra: 1. the mean of the selected acquisitions, 2. the mean of the selected acquisitions reconstructed with  $M$  independent components and 3. the mean of the selected acquisitions reconstructed with only the main independent component. The latter spectrum corresponds to the scaled main independent component. The application of ICA and the identification of the non-distorted ICA component are novel in this context.

### *Noise and SNR analysis*

In principle, noise can be estimated at one frequency by determining the standard deviation of the selected acquisitions and dividing by the square root of the number of acquisitions. Possibly only few acquisitions may be left, and this will make this noise estimation unreliable. However this is not a problem with the datasets used as completely corrupted data was excluded. Noise will be underestimated, however, since the standard deviation is minimized for the outlier identification methods. This is most prominent for the algorithm without connection between the Fourier components (the frequency direction). The ICA method does not have this problem, but the independent components have a lower noise than the original acquisitions. For ICA, the noise at each particular frequency can be determined by resampling with the JackKnife (29) method, but in order to aid comparison an identical noise estimation procedure for all motion-rejection algorithms is preferred. Since there are no metabolite signals between 8 and 9 ppm, this part of the spectrum is used for estimating the noise. The standard deviation of the final signal is determined over this frequency range, which does not depend on the number of selected acquisitions. It is assumed that the signal is constant in this part of the spectrum and that the noise is independent of frequency.

For the Signal-to-Noise Ratio (SNR) and signal analysis, the signal is regarded as the peak height of the three main metabolite peaks, N-acetyl aspartate at 2.02 ppm, creatine at 3.04 ppm and choline at 3.24 ppm. Both mean peak height and average SNR of these three peaks were calculated for each dataset. In order to be able to compare between subjects, both signal and SNR were normalized by the values for the mean filtered signal. The algorithm with both the highest signal and highest SNR is considered as the optimal algorithm. Since position change is a source of erroneous measurements and causes simultaneous broadening and lowering of peaks, the area under the metabolite peak is not a proper measure of the quality of the measurement.

Acceptance percentage for each algorithm and each dataset was defined by the number of single data points that were not rejected by the algorithm as a percentage of the total number of data points. The total number of data points equals the number of repetitions times the number of Fourier components.

## Results

The first dataset of the healthy volunteer had 48 comparable spectra and the ICA algorithm found only one component, as is expected for a dataset without motion. The effect of (instructed) motion on the other two datasets of the volunteer was comparable. Figure 1 shows the spectrogram (top panel) and the coefficients for the components (bottom panel) of the second dataset, where the healthy volunteer was instructed to move his head at certain times. The influence of head movement is clearly seen in the spectrogram, and ICA components describe the different periods. A typical result for measurement of a preterm infant that has been hampered by motion is shown in figures 2 to 6. The top panel in figure 2 shows the spectrogram for short echo time, and the bottom panel shows the coefficients for the components in the ICA algorithm. Figures 3 and 4 show the final spectra between 2.8 and 3.5 ppm for all algorithms for an 8 mL voxel with short echo time (fig. 3) and long echo time (fig. 4). Figure 5 shows the entire short-echo-time spectrum. The noise is estimated from the signal between 8 and 9 ppm, since there are no metabolite signals there. Figure 6 shows the short-echo-time spectrum around the residual water peak and the removal of a water peak erroneously displaced by subject movement. Both peak heights and SNR for the three main metabolite peaks behave comparably, so only the average signal and SNR for the three metabolite peaks are discussed, and referred to as “the signal” and “the SNR”. The SNR of the mean filtered spectra ranged from 8.4 to 54.3, and was highest for the 8 mL voxel with short echo time and lowest for the 3.4 mL voxel with long echo time. The SNR was (mean  $\pm$  standard deviation)  $29.9 \pm 8.3$  for the 8 mL voxel with short echo time and  $15.1 \pm 5.1$  the 3.4 mL voxel with long echo time.

The Signal and the SNR relative to the signal, as well as the SNR of the mean of all repetitions (both defined as 1) for all motion-rejection algorithms with and without non-motion-distorted acquisitions are shown in table 1. The acceptance percentage, defined as the percentage of the data points that is accepted by the algorithms described in the methods section, is shown in the last column. The values for the subset of the datasets where ICA detected more than one component are given in brackets. The values for the signal, the SNR and the acceptance percentage in table 1 are averaged over all datasets. All motion-rejection algorithms improve the signal and remove movement artifacts. The results for the dataset of the healthy volunteer, see figure1, were similar to the results in table 1.

Both the signal and the SNR were statistically tested bilaterally between all methods with a paired, double-sided t-test. Apart from the difference in the signal for the two outlier identification methods (point wise OI and OI), all the differences in the signal and the SNR in table 1 are significant ( $p < 0.05$ ) for all datasets.

**Table 1:** The mean signal (here “signal” is defined as the average height of the NAA, Cho and Cr peaks), SNR and acceptance percentage for all datasets. Between brackets the values for the subset of datasets where ICA detects more than one component, i.e. with motion artifacts, are shown. Signal and SNR are stated relative to the signal and SNR of the mean of all acquisitions.

Method	Signal	SNR	acceptance percentage
mean	1	1	100
median	1.030 (1.036)	0.849 (0.866)	100
pointwise OI	1.066 (1.082)	0.739 (0.758)	85.3 (84.8)
OI	1.069 (1.106)	0.939 (0.948)	75.7 (70.6)
ICA mean	1.114 (1.201)	0.950 (0.912)	75.4 (56.7)
ICA all components	1.100 (1.178)	0.976 (0.957)	75.4 (56.7)
ICA main component	1.088 (1.158)	0.970 (0.945)	75.4 (56.7)

#### *ICA and components*

138 out of 243 subject spectra (each containing 48 acquisitions) contained more than one component. So in 105 subject spectra the ICA algorithm finds only one component, and identifies differences between this component and the measured signal as noise. The probability of having estimated the correct number of components was less than 100% for 30 of these patient spectra (ranging from 50 to 99%). Of the 138 spectra with more than one component, 43% of the measurements were rejected. The average number of components was 3.2 (range 1-12, the maximum number of components was set to 12) for all measurements and 3.6 (range 2-12) for the motion-distorted measurements. On average 75% of all the measurements were kept.

## Discussion

Motion compensation of SVS spectra of non-anesthetized infants and other moving patients is necessary. The effect of motion on the spectrogram of the healthy volunteer in figure 1 showed that spectra are corrupted during motion and that the frequency of the metabolite peaks is shifted after motion due to a change of voxel position. During motion of the healthy volunteer the water peak was reduced while it was increased in the preterm infant. A signal loss as seen in the volunteer spectrum is expected due to imperfect refocusing when motion happens during the spin-echo period of the sequence. A signal increase as seen in the infant spectrum is expected when the water suppression is compromised by movement. The proposed methods detect and compensate both effects.

Visual inspection of the spectra indicates higher signals and better spectral resolution for all the motion-rejection algorithms. In practice it is not possible to visually appreciate the noise properties of the algorithms, for instance by observing the signal where no metabolite peaks are present in figure 3. Visual inspection also indicates that the ICA methods are better at suppressing the signal just next to the metabolite peaks and that median filtering does not completely remove the influence of outliers, resulting in a lower signal at the metabolite peaks.

Because motion is likely to reduce the peak height, the signal and the SNR are reasonable measurements for the performance of the algorithms, although since true metabolite concentrations are not known, the true performance is also not known. Simulations could be performed to address the issue of the true performance of the algorithms.

If SVS with a relatively large voxel of more than 1 mL is used to measure a “global” metabolite concentration, small changes in which the voxel stays within the same tissue of interest are less relevant than in the case where a small voxel is used and a spectrum at a specific position, e.g. the hippocampus, is required. In the latter case it is advisable to perform a localizer scan before and after the spectroscopy measurement in order to ensure that the voxel position is not changed, even though the acquired spectra are not noticeably different. If the exact voxel position is very important, the selection of the ICA component can be altered by identifying the undistorted component as the dominant component of the first acquisition instead of the most frequent dominant component. In this way the ICA algorithms reject acquisitions that differ significantly from the first acquisition. It is also possible to reject all acquisitions after the first detected movement. On the other hand the selection of the acquisitions in the ICA method only accepts

acquisitions which differ by the ICA-identified noise, which indicates that the underlying noiseless spectrum is unchanged by motion, and that the head has therefore probably returned to the original position after motion.

Quantitative evaluation shows that median filtering results in a considerable improvement of the signal and compensation for movement-distorted spectra. However, it does not perform as well as the other methods, and the SNR is reduced by more than 15% compared to the uncorrected mean signal, although the mean signal may, however, be corrupted. A combination of order-statistics filters such as All-Rank Selection Order-Statistics filtering (30) might reduce noise and outlier sensitivity compared to median filtering, but this has not been shown. Pointwise outlier identification has even lower SNR, but slightly better signal amplitude compared to the median filter. Outlier identification with connection between the consecutive Fourier components did not give this SNR loss and restored the signal well. The relatively conservative  $p$ -value for the pointwise outlier identification method is necessary, as otherwise too many measurements will be excluded. The outlier identification method with multiple comparisons, however, needs a slightly higher  $p$ -value in order to reject enough measurements.

The noise depends on the algorithm and it increases if the number of accepted acquisitions  $n$  is lower and is proportional to  $1/\sqrt{n}$ . The signal is increased if the motion-distorted acquisitions are rejected, and the SNR is reduced less than expected from the increase in noise only. In general the noise in the median is higher than the noise in the mean. For normal distributions this is approximately 25%. The SNR is only 15% lower for the median and this is due to the fact that the median recovers the signal better than the mean. As an estimator, the median is more sensitive to noise, and therefore it is probably better to identify the outliers, reject them, and calculate the mean of the remaining data. Outlier identification with multiple comparisons performs better than the median, but the pointwise outlier identification method does not. This is probably because of the noise sensitivity of the (pointwise) outlier detection itself.

The advantages of ICA compared with the other methods are that no arbitrary thresholds need to be set, that both the resulting signal and the SNR are best, and that it provides a possibility to identify outliers without ignoring connections between consecutive Fourier components. Another advantage of the ICA methods is that they make it possible to accept all the measurements if just one component is considered as most probable, for instance if the patient does not move. Also the range of the acceptance-rate-defined percentage of the measurements which are not rejected

indicates larger flexibility. The standard deviation of the acceptance rate considering both movement-distorted and undistorted data for ICA was 25%, while it was 11% for outlier identification and only 1.5% for pointwise outlier identification. The latter is explained by the influence of the majority of the Fourier components, where no metabolite signal is present. The difference between the three versions of the ICA method was small. Using ICA only to identify movement-distorted acquisitions, and then taking the mean of the remaining acquisitions gives the highest signal. On the other hand, taking the mean of signals reconstructed with the main or all components showed slightly better SNR.

In the case of a short movement, it is possible that the first few measurements after the movement are transients due to history effects in the spin system. ICA will describe this transition with two or more components. Hereafter the measurement is described with one component, different from the component found before movement, unless the subject returned to the original position.

Independent Component Analysis (ICA) instead of the better known Principal Component Analysis (PCA) is used, because the latter maximizes the explained variance for each component, i.e. minimizing the mean square error of approximating the data, whereas ICA seeks independent components. In the case of a measurement with some motion-distorted acquisitions, PCA finds a mixture of all acquisitions for the first and other components (often after the mean has been subtracted), and because of the large deviations in the motion-distorted acquisitions, the uncorrelated principal components will be mainly determined by distorted acquisitions. This gives no opportunity to identify the motion-distorted acquisitions, while ICA finds the undistorted acquisitions as one independent component, and one or more components for the motion-distorted acquisitions.

Phase-coherent averaging after motion rejection will probably increase the SNR even more, but caution is necessary, since it can potentially introduce a bias. In this study no phase-coherent averaging was applied, because only the performance of the motion rejection algorithms was investigated.

## **Conclusion**

Subject movements cannot be ignored in certain patient groups and they need to be compensated for. This can be done by storing the individual SVS acquisitions and identifying and rejecting the acquisitions distorted by subject movements followed by phase correcting (and optionally frequency shift compensating) the individual remaining acquisitions before averaging. It is strongly advised to implement a procedure to detect subject motion. A first implementation of motion rejection in clinical practice could be to monitor the difference between the mean and the median and compare this with the estimated noise. If the difference is significant, the median instead of the mean should be used, or outlier identification or ICA analysis could be applied to the dataset.

Fully automated ICA analysis proved to be the most powerful and reliable tool for movement identification and rejection. In this study the signal increased by 20% for the subject-movement-distorted data, keeping the SNR as high as 91% of the SNR of the mean signal and keeping the undistorted patient data unaffected.

## **Acknowledgment**

This work was partly funded by the Danish Medical Research Council.

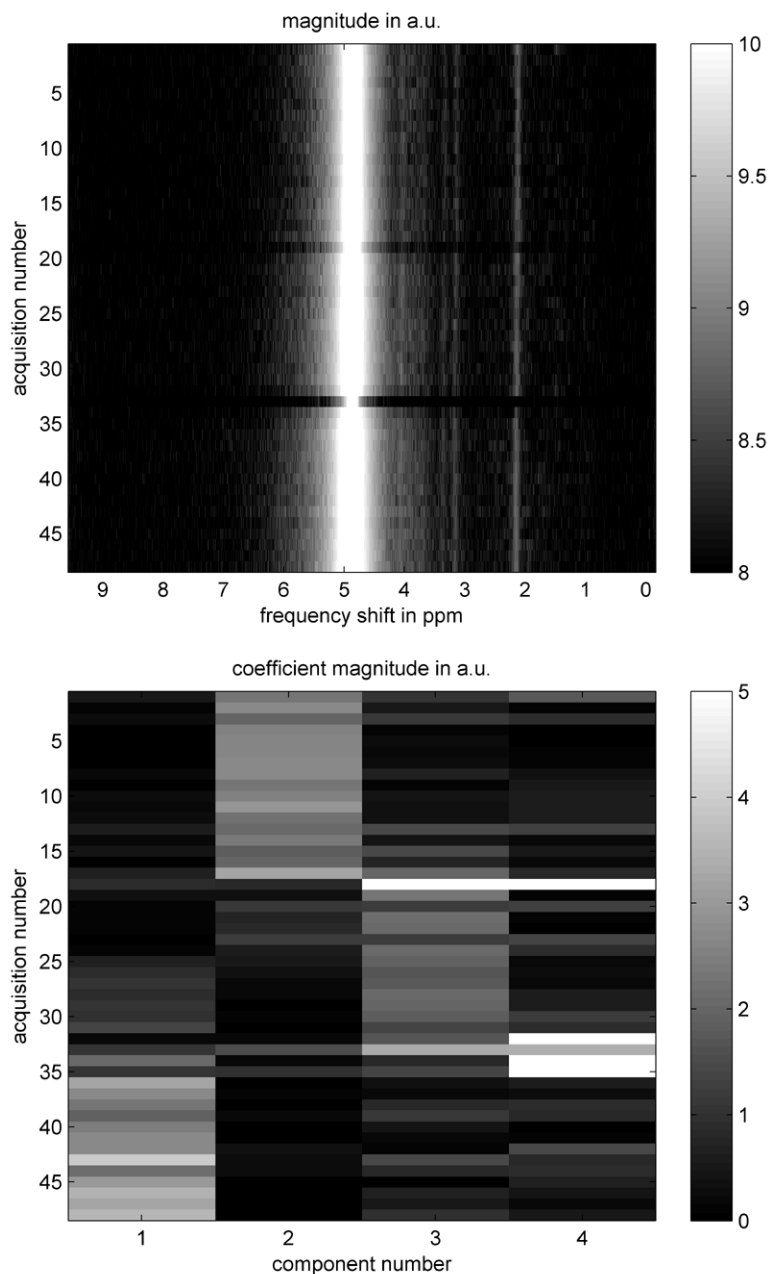


**Figure 1:** The spectra of 48 acquisitions of an 8 mL voxel with an echo time of 30 ms for a healthy volunteer (top panel). The volunteer was instructed to move his head 2-3 cm continuously from the left to the right at acquisitions 18-19, and 32-34. Each spectrum is shown as a row using the grayscale for the log of the magnitude of the signal intensity in arbitrary units (a.u.). The residual water peak at 4.7 ppm is clearly visible, as are metabolite signals at the right hand side of the water peak. In the bottom panel, the coefficients for the ICA components for the spectra are shown. A grayscale is used to show the amplitude of the coefficients in a.u. The three periods without movement are mainly described by a single component for each period (component 2-3-1), while the spectra during head movement are described by a combination of all four components.

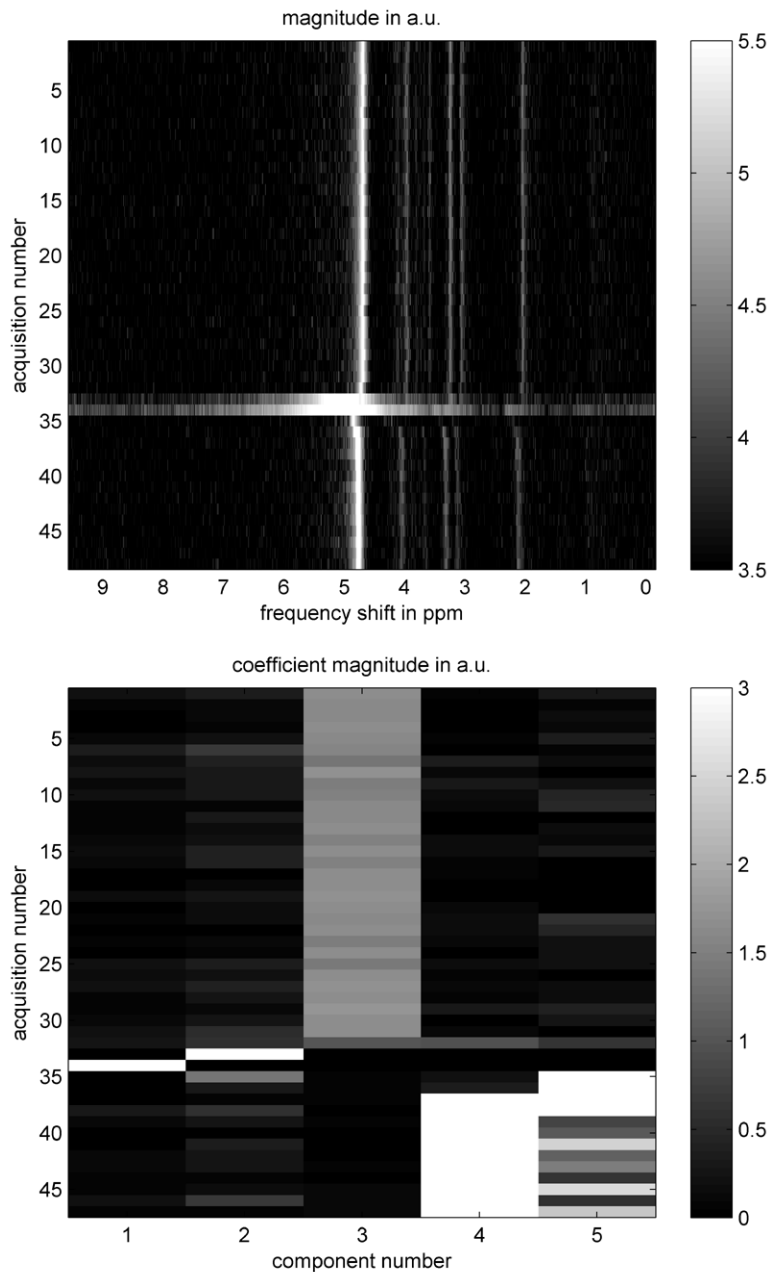


**Figure 2:** The spectra of 48 acquisitions of an 8 mL voxel with an echo time of 30 ms for a preterm infant (top). Acquisitions number 33 and 34 are likely to be corrupted by motion, while acquisitions 35 to 48 are likely to be measured at another position (the spectrum is slightly shifted) and should be rejected. In the bottom panel, the coefficients for the ICA components for the spectra are shown. In this case the most frequent dominant component is component 3, and it is interpreted by the ICA algorithm as the undistorted component. Components 1 and 2 describe acquisitions 33 and 34, which are interpreted as motion corrupted, see top panel. Components 4 and 5 describe the acquisitions 35 to 48. Notice that component 3 almost solely describes the undisturbed data.

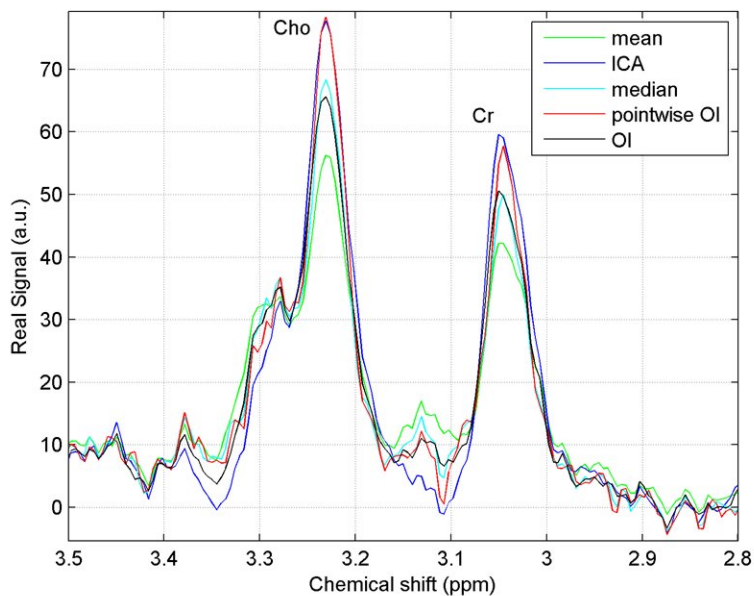


**Figure 3:** A part of the zero-order phase-corrected spectrum for a 30 ms echo time after motion rejection with the creatine peak at the right and choline peak at the left. On the left shoulder of the choline peak the myo-inositol resonance at 3.28 ppm is visible. The curves illustrate the performance of the different algorithms, mean, ICA, median, pointwise outlier identification (pointwise OI) and outlier identification (OI). It is clearly seen that the median improves the signal, and that in this case pointwise OI and ICA perform best in agreement with quantitative analysis.

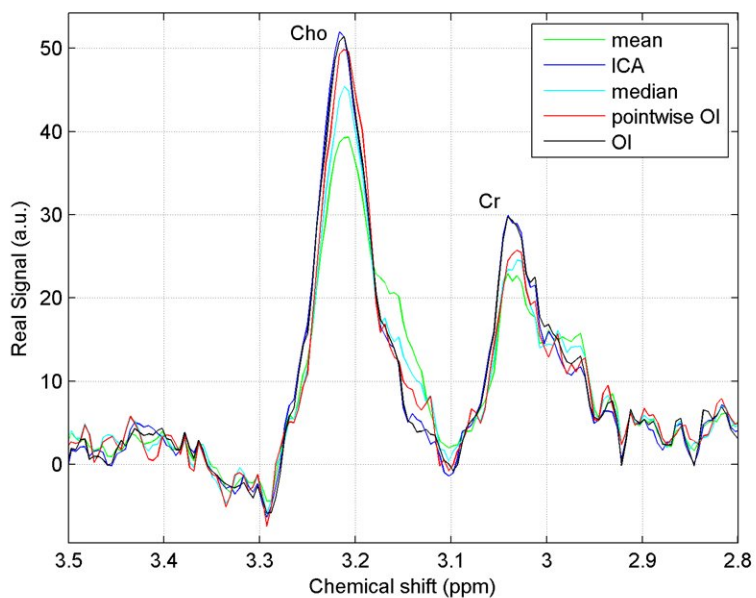


**Figure 4:** Graph similar to figure 3, but based on data acquired with an echo time of 144 ms. It is seen that the median improves the signal, that pointwise OI performs better, and that in this case ICA and OI perform best in agreement with quantitative analysis.

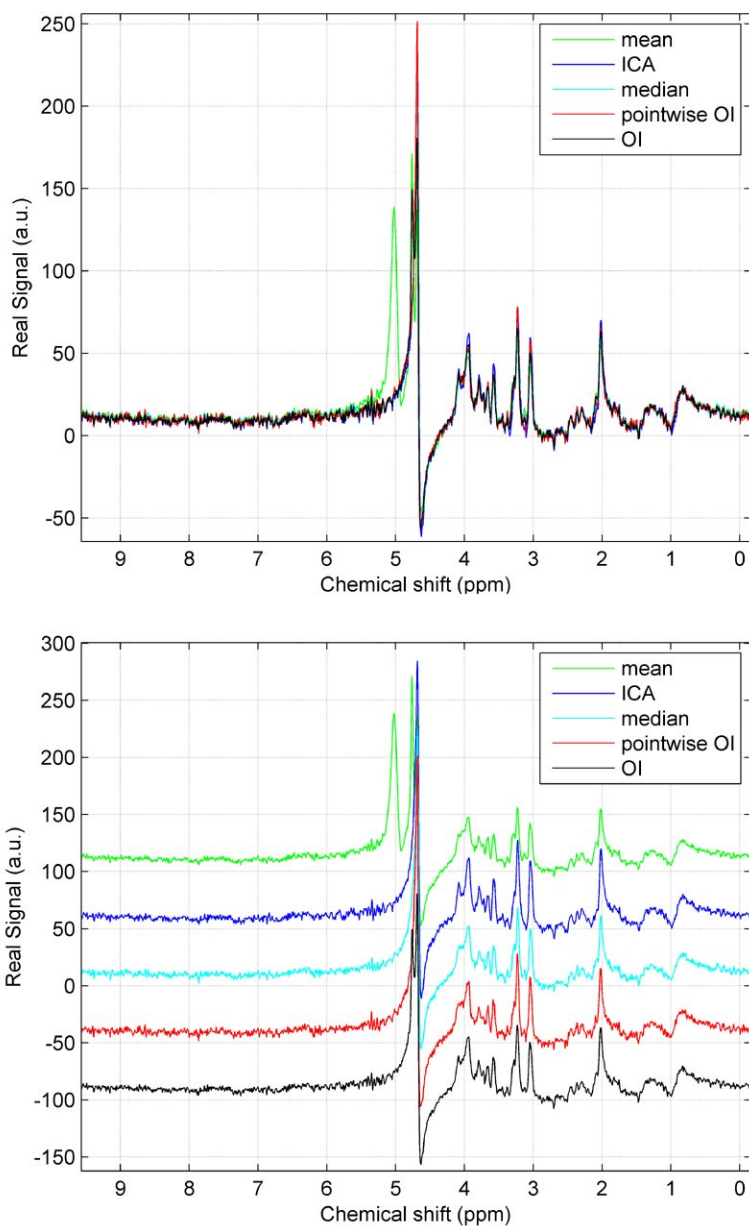


**Figure 5:** Entire water-suppressed spectra acquired with an echo time of 30 ms for the same subject as in figure 3. The residual water peak at 4.7 ppm is clearly seen. Peaks in the mean signal (green) at 5.1 and 4.8 ppm originate from the residual water signal and subject motion.

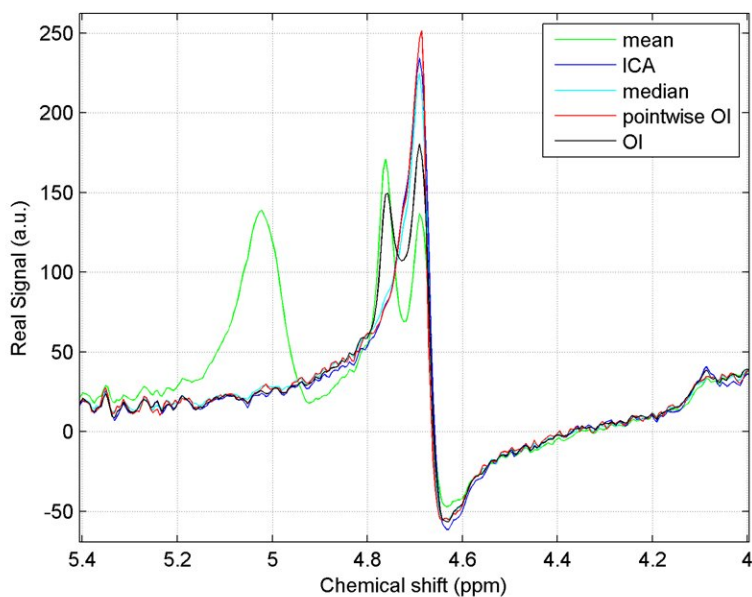


**Figure 6:** The 1.4 ppm frequency range around the residual water peak acquired with an echo time of 30 ms for the same subject as in figure 3. The residual water peak at 4.7 ppm is clearly seen. Peaks in the mean signal (green) at 5.1 and 4.8 ppm originate from the residual water signal and subject motion. All motion rejection algorithms remove these erroneous water peaks, except the outlier identification with multiple comparisons that fails to remove the peak at 4.8 ppm.

## References

1. Drost DJ, Riddle WR, Clarke GD. Proton magnetic resonance spectroscopy in the brain: report of AAPM MR Task Group #9. *Med Phys.* 2002;29(9):2177-97. Review.
2. Jansen JF, Backes WH, Nicolay K, Kooi ME. 1H MR spectroscopy of the brain: absolute quantification of metabolites. *Radiology* 2006;240(2):318-32. Review.
3. Felblinger J, Kreis R, Boesch C. Effects of physiologic motion of the human brain upon quantitative 1H-MRS: analysis and correction by retro-gating. *NMR Biomed.* 1998;1(3):107-14.
4. Katz-Brull R, Rofsky NM, Lenkinski RE. Breathhold abdominal and thoracic proton MR spectroscopy at 3T. *Magn Reson Med.* 2003;50(3):461-7.
5. Katz-Brull R, Lenkinski RE. Frame-by-frame PRESS 1H-MRS of the brain at 3 T: the effects of physiological motion. *Magn Reson Med.* 2004;51(1):184-7.
6. Zhu G, Gheorghiu D, Allen PS. Motional degradation of metabolite signal strengths when using STEAM: a correction method. *NMR Biomed.* 1992;5(4):209-11.
7. Helms G, Piringer A. Restoration of motion-related signal loss and line-shape deterioration of proton MR spectra using the residual water as intrinsic reference. *Magn Reson Med.* 2001;46(2):395-400.
8. Bolan PJ, Henry PG, Baker EH, Meisamy S, Garwood M. Measurement and correction of respiration-induced B0 variations in breast 1H MRS at 4 Tesla. *Magn Reson Med.* 2004;52(6):1239-45.
9. Shanbhag DD, Dunham SA, Knight-Scott J. A water signal based navigation echo for localized MRS In Proceedings of the 13th Annual Meeting of ISMRM, Miami Beach, Florida, USA, 2005, p. 2505.
10. Thiel T, Czisch M, Elbel GK, Hennig J. Phase coherent averaging in magnetic resonance spectroscopy using interleaved navigator scans: compensation of motion artifacts and magnetic field instabilities. *Magn Reson Med.* 2002;47(6):1077-82.
11. Bhattacharyya PK, Lowe MJ, Phillips MD. Spectral quality control in motion-corrupted single-voxel J-difference editing scans: an interleaved navigator approach. *Magn Reson Med.* 2007;58(4):808-12.
12. Pfeuffer J, Juchem C, Merkle H, Nauerth A, Logothetis NK High-field localized 1H NMR spectroscopy in the anesthetized and in the awake monkey. *Magn Reson Imaging.* 2004;22(10):1361-72.
13. Skimminge A, Markenroth K, Hejl A, Hanson LG. Improved spectroscopy using cluster analysis and lipid signals as a motion indicator. In Proceedings of the 11th Annual Meeting of ISMRM, Toronto, Ontario, Canada, 2003, p. 270.
14. Gabr RE, Sathyanarayana S, Schär M, Weiss RG, Bottomley PA. On restoring motion-induced signal loss in single-voxel magnetic resonance spectra. *Magn Reson Med.* 2006;56(4):754-60.
15. Bottomley PA. Spatial localization in NMR spectroscopy in vivo. *Ann N Y Acad Sci.* 1987;508:333-48.
16. Slotboom J, Nirkko A, van Ormondt D. A Comparison of Time Domain and Frequency Domain All Rank Selection Order Statistics Filtering (ARSOS) of Single Voxel 1H MRS-signals. In Proceedings of the 15th Annual Meeting of ISMRM, Berlin, Germany, 2007. p. 203.

17. Slotboom J, van Ormondt D, Brekenfeld C, Nirikko A, Schroth G. The usage of median filtering for the elimination of patient motion related signal artifacts in single voxel spectroscopy. In Proceedings of the 22nd Annual Scientific Meeting of ESMRB, 2005, Basle, Switzerland. p. 124-125.
18. Slotboom J, van Ormondt D. Elimination of Patient-Motion Artefacts in In Vivo MR Spectroscopy. In Proceedings of ProRISC, IEEE Benelux, Veldhoven, The Netherlands, 2006, p. 204-207.
19. Rider PR. Variance of the Median of Small Samples from Several Special Populations J. Amer. Statist. Assoc. 1960;55:148-150.
20. Kenney, J. F. and Keeping, E. S. The Median, Relation Between Mean, Median, and Mode, Relative Merits of Mean, Median, and Mode, and The Median. In: Mathematics of Statistics, Pt. 1, 3rd ed.; 1962, p. 211.
21. Balakrishnan N, Rao CR. Order-statistic filtering and smoothing of time-series: Part II. In Handbook of Statistics 17: Order Statistics: Applications, Elsevier; 1998, p. 555-602.
22. Thomsen G, de Nijs R, Høgh-Rasmussen E, Frokjaer V, Svarer C, Knudsen GM. Required time delay from (99m)Tc-HMPAO injection to SPECT data acquisition: healthy subjects and patients with rCBF pattern. Eur J Nucl Med Mol Imaging 2008;35(12):2212-2219.
23. Andersson JLR. How to estimate global activity independent of changes in local activity. Neuroimage 1977;60:237-244.
24. Bell A, Sejnowski TJ. An Information-Maximization Approach to Blind Separation and Blind Deconvolution. Neural Computation 1995;7:1129-1159.
25. Højen-Sørensen P, Hansen LK, Winther O. Mean Field Implementation of Bayesian ICA. In proceedings of the 3rd International Conference on Independent Component Analysis and Blind Signal Separation, San Diego, USA, 2001, p. 439-444.
26. Hyvärinen A, Oja E. Independent component analysis: algorithms and applications. Neural Netw. 2000;13:411-30.
27. Kolenda T, Hansen LK, Larsen J. Signal detection using ICA: application to chat room topic spotting. In proceedings of the 3rd International Conference on Independent Component Analysis and Blind Signal Separation, San Diego, USA, 2001, p. 540-545.
28. Hansen LK, Larsen J, Kolenda T. Blind Detection of Independent Dynamic Components. In Proceedings of IEEE International Conference on Acoustics, Speech, and Signal Processing (ICASSP), 2001;5, p. 3197-3200.
29. Miller RG. The Jackknife--A review. Biometrika 1974;61(1):1-15.
30. Slotboom J, van Ormondt D. The Effect of Order-Statistics Filtering on the Output Probability Density Functions. In Proceedings of ProRISC, IEEE Benelux, Veldhoven, The Netherlands, 2007, p. 254-258.

## Footnotes

1. Kolenda T, Sigurdsson S, Winther O, Hansen LK, Larsen J. DTU:Toolbox, Intelligent Signal Processing group at the Institute of Informatics and Mathematical Modelling at the Technical University of Denmark, 2002, <http://isp.imm.dtu.dk/toolbox/>